

Supporting information

Synchronous oil/water separation and wastewater treatment on a copper-oxide-coated mesh

Yahua Liu¹, Peng Xu¹, Wenna Ge¹, Chenguang Lu¹, Yunlai Li¹, Shichao Niu², Junqiu Zhang², Shile Feng^{1*}

¹Key Laboratory for Precision & Non-traditional Machining Technology of Ministry of Education, Dalian University of Technology, Dalian 116024, China

²Key Laboratory of Bionic Engineering, Ministry of Education, Jilin University, Changchun 130022, China

*Correspondence should be addressed to S.F. (fengshile@dlut.edu.cn).

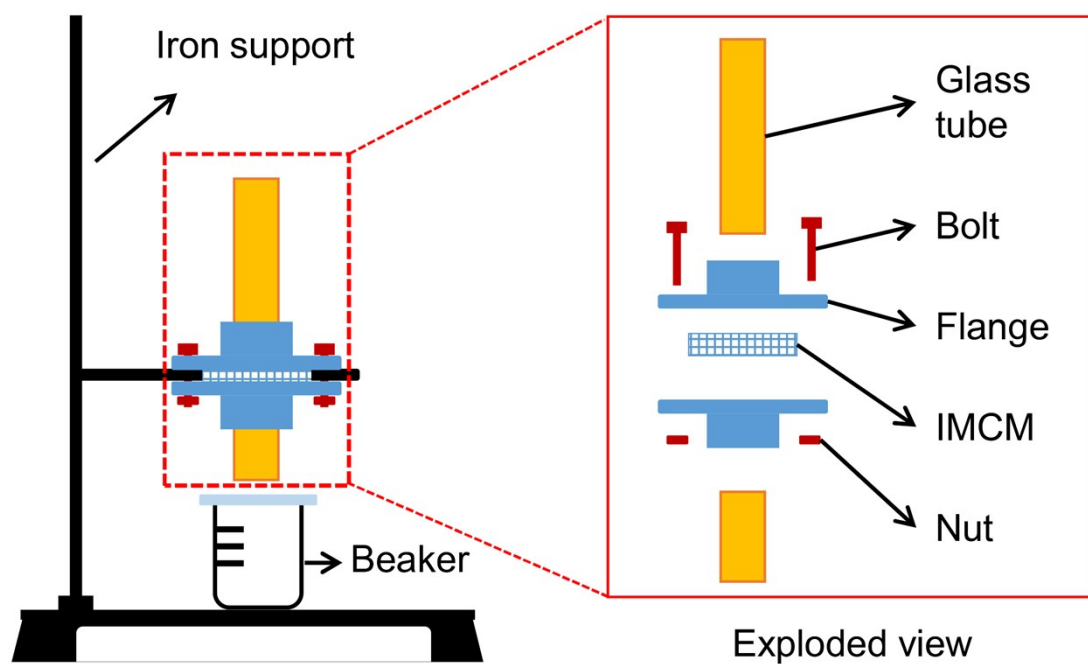


Figure S1. The schematic of oil/water separating device. The IMCM is clamped between two flanges by four bolts while two glass tubes are fixed in the grooves of the flanges. The oil/water mixture is poured into the upper glass tube and the water is collected by the beaker below.

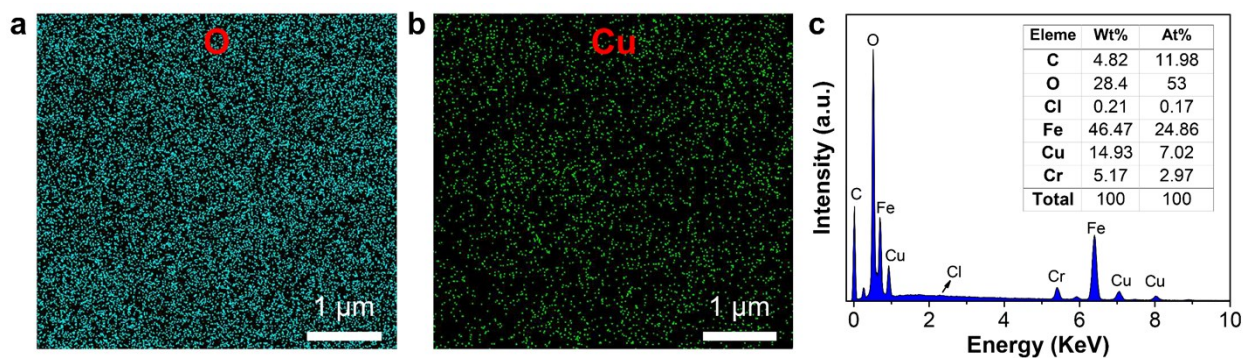


Figure S2. The EDS images of the IMCM with $w = 5\%$. (a) The EDS mapping of O element. (b) The EDS mapping of Cu element. (c) The EDS spectrum of the IMCM. The contents of all the elements are described as the table.

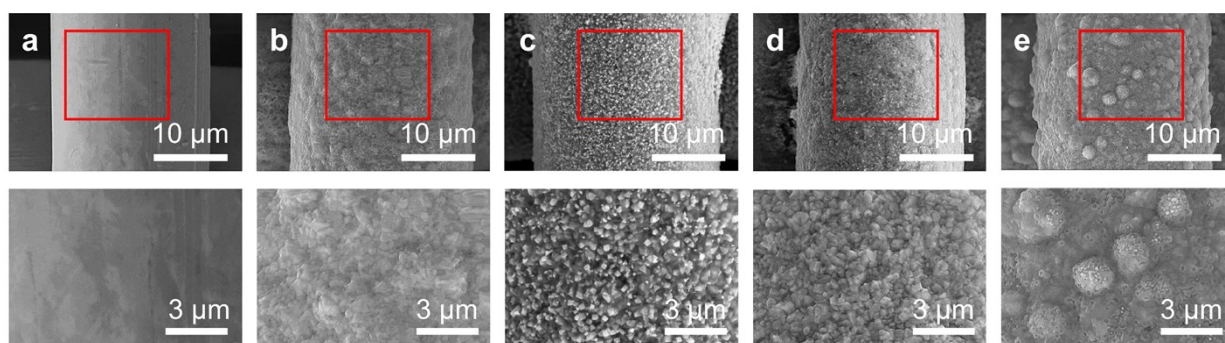


Figure S3. The morphology structures of different IMCM. (a) The SEM images of the IMCM with $w = 0\%$. (b) The SEM images of the IMCM with $w = 1\%$. (c) The SEM images of the IMCM with $w = 3\%$. (d) The SEM images of the IMCM with $w = 5\%$. (e) The SEM images of the IMCM with $w = 7\%$.

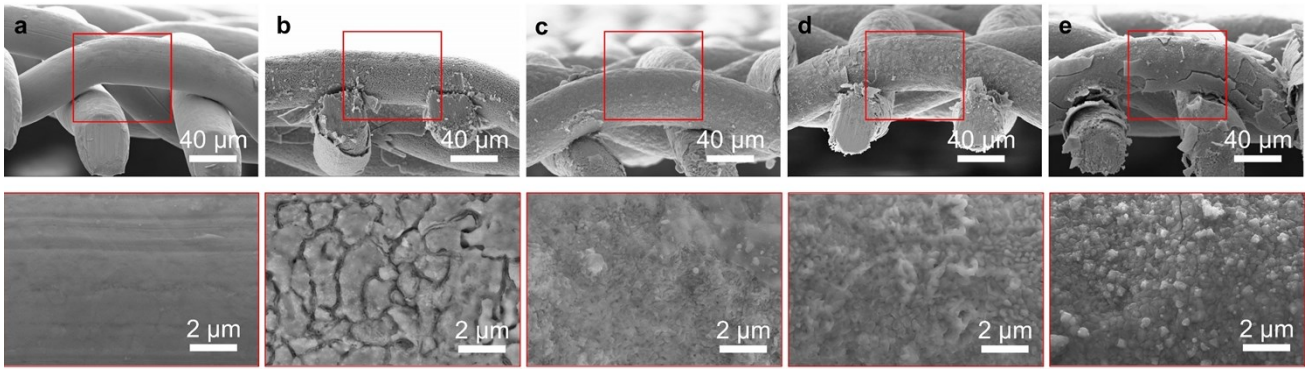


Figure S4. The morphology structures on the cross section of IMCM. (a) The cross-section images of the IMCM with $w = 0\%$. (b) The cross-section images of the IMCM with $w = 1\%$. (c) The cross-section images of the IMCM with $w = 3\%$. (d) The cross-section images of the IMCM with $w = 5\%$. (e) The cross-section images of the IMCM with $w = 7\%$.

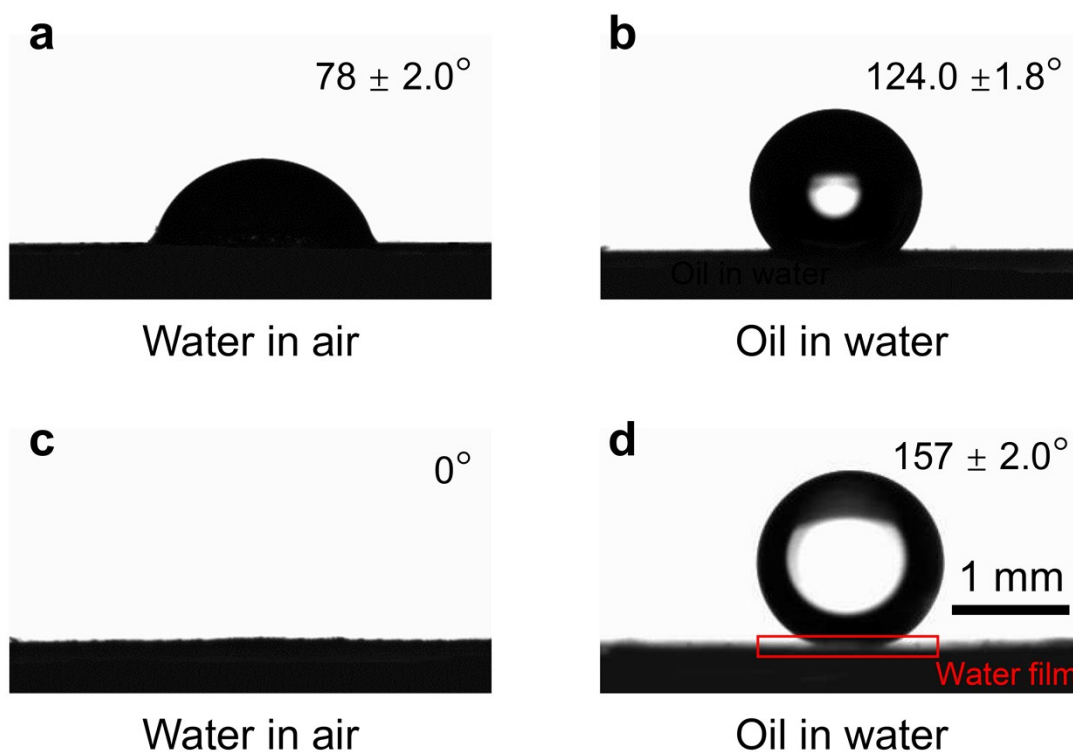


Figure S5. The wettability of different IMCM surfaces. (a) The contact angle of a water droplet on the IMCM surface with $w = 0\%$ in air. (b) The contact angle of an oil droplet on the IMCM surface with $w = 0\%$ underwater. (c) The contact angle of a water droplet on the IMCM surface with $w = 5\%$ in air. (d) The contact angle of an oil droplet on the IMCM surface with $w = 5\%$ underwater. The volume of the droplet is $3 \mu\text{L}$.

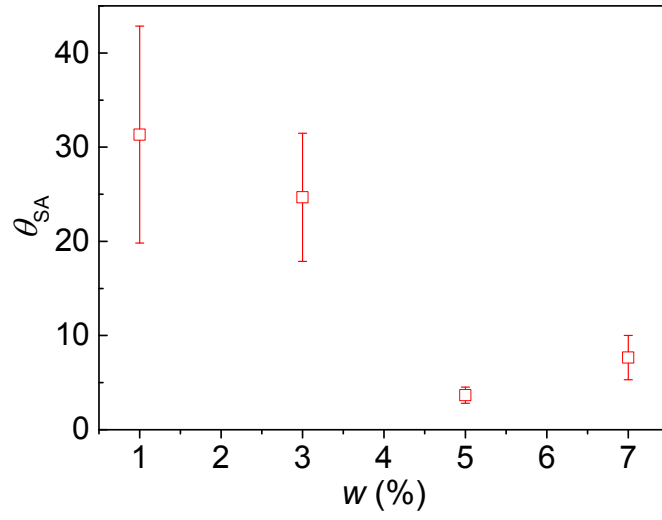


Figure S6. Sliding angles of oil (dichloroethane) droplet on IMCM treated with different w underwater. For $w < 5\%$, $\theta_{SA} > 20^\circ$ and for $w \geq 5\%$, $\theta_{SA} < 10^\circ$. The results shows that IMCM treated with $w \geq 5\%$ manifests superoleophobicity and low-adhesion underwater.

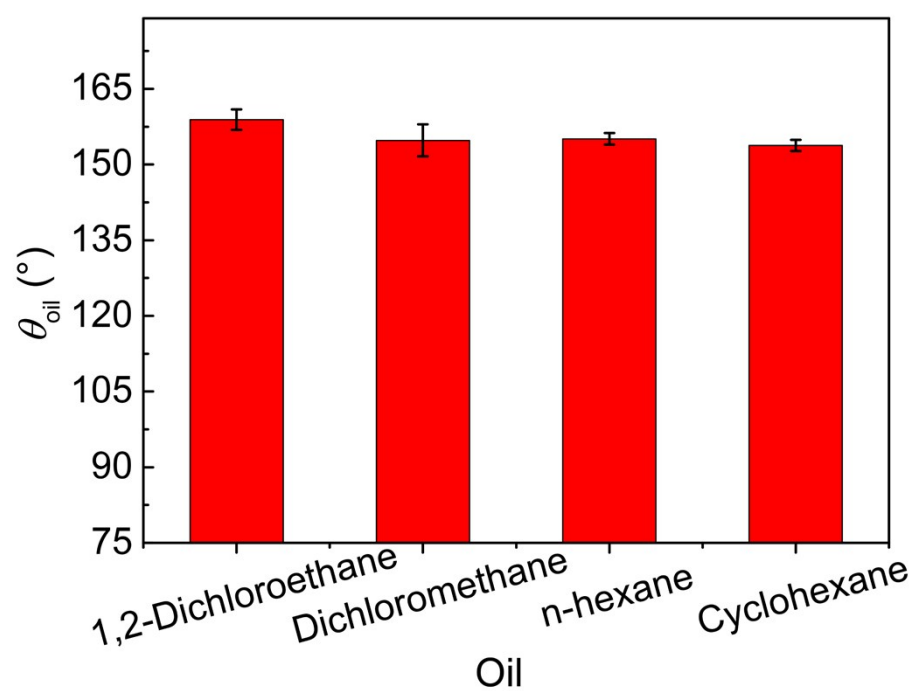


Figure S7. The contact angle of different types of oils on the IMCM surfaces with $w = 5\%$.

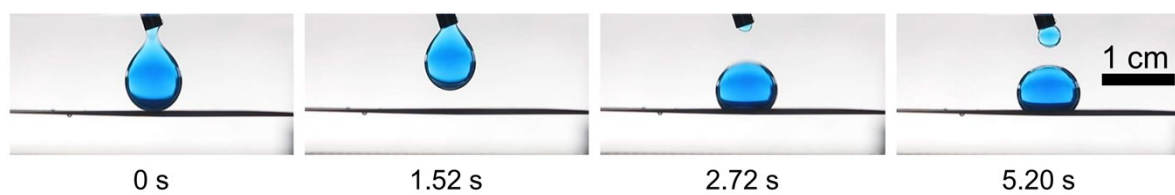


Figure S8. Dynamic test of water droplets impacting on the IMCM with $w = 5\%$ without pre-wetting under oil (liquid paraffin) environment. The water droplet could not spread on the surface and the methylene blue in water droplet could not be catalytically degraded.

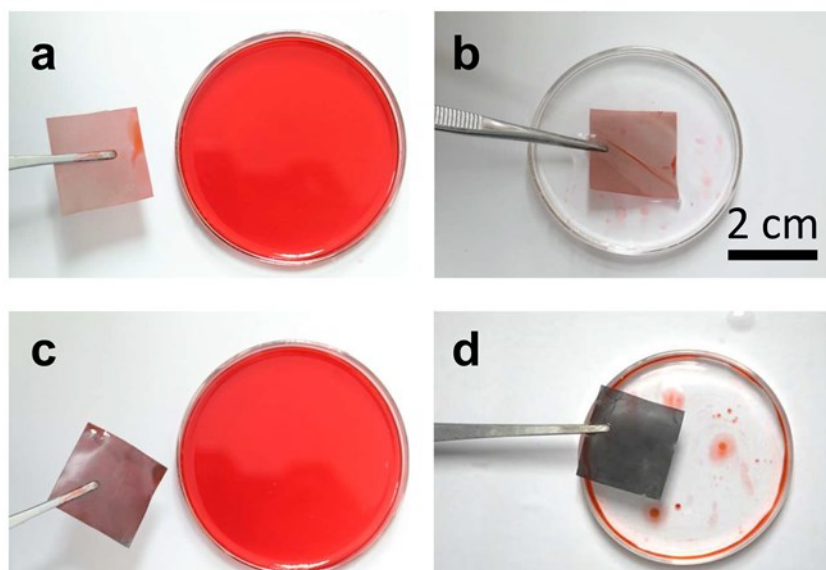


Figure S9. The self-cleaning property test of IMCM. (a) The image of the IMCM with $w = 0\%$ after immersing into the oil. (b) The image of the prewetted IMCM with $w = 0\%$ contained with oil after immersing in the water. There was still some oil contamination on the surface of the mesh. (c) The image of the prewetted IMCM with $w = 5\%$ after immersing into the oil. (d) The image of the IMCM with $w = 5\%$ contained with oil after immersing in the water. The surface of the mesh is clean.

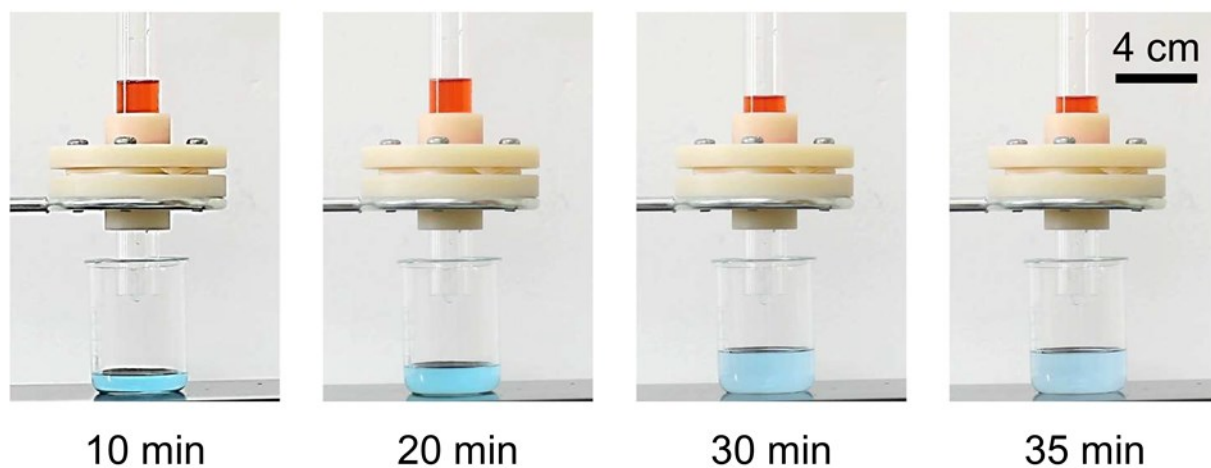


Figure S10. The catalytic degradation performance of IMCM with $w = 0\%$. After 35 minutes, the color of the water collected was still blue.

Table S1 The measured value of breakthrough pressure for different oils

Oils	Oil-water interfacial force (mN/m)	OCA (°)	Breakthrough pressure(kPa)
n-hexane	51.1	156.7	2.03
diesel	30.3	154.1	1.20
dichloroethane	27.9	158.2	1.11
toluene	36.1	155.0	1.43